Computational fluid dynamics simulation of laboratory scale reactor of fast pyrolysis fluidised bed

2017 J. Phys.: Conf. Ser. 822 012028

(http://iopscience.iop.org/1742-6596/822/1/012028)

Computational fluid dynamics simulation of laboratory scale reactor of fast pyrolysis fluidised bed

Seyed Amirmostafa Jourabchi[1*], Hoon Kiat Ng[2], Suyin Gan[2] and Zhong Jian Tan[1]

[1] Faculty of Engineering and Quantity Surveying, INTI International University, Jalan BBN 12/1, Bandar Baru Nilai, 71800 Nilai, Negeri Sembilan, Malaysia
[2] Faculty of Engineering, The University of Nottingham Malaysia Campus, Jalan Broga, 43500 Semenyih, Selangor, Malaysia

E-mail: * amir.jourabchi@newinti.edu.my

Abstract. Euler-Eulerian two-fluid model (EE-TFM), among the computational fluid dynamics (CFD) techniques and module available on the market, have been chosen to study and obtain the operational parameters required for the fluidisation of different materials and different particle diameters of the fluidised bed model. In the present work, the effect of the material, namely stainless steel and sand with the respective diameters of 0.5 and 1 mm have been investigated with the aid of ANSYS FLUENT 15. From the simulation, it has found that the minimum required superficial velocity of the driving gas for fluidisation of steel beads are 70 cm/s and 140 cm/s respectively for diameter of 0.5 and 1.0 mm. On the other hand, the minimum required superficial velocities to fluidise the less dense sand beads are 30 cm/s and 70 cm/s for particle diameter of 0.5 and 1.0 mm respectively. The results show that the minimum fluidisation velocity increases as the density of the particle material increases; while it also increases, when the particle diameter increases. It is concluded that the drag force required to fluidise the specific solid bead material is proportional to both the density and the diameter of the particle chosen.

1. Introduction

In 2010, the global production of biofuel has exceeded over 100 billion litres, comparing to the previous year, it has rose by approximately 17% [1]. The trend has shown that many nations are driven to invest more on the renewable energy, namely biofuel. Glancing through the public concern regarding the human strong dependency on fossil fuels and its insecure supply, biofuel has turned out to be an alternative to reduce the consumption of fossil fuels for transportation need. However, it is crucial to ensure that the demand for biomass does not compete with the regional food supplies, such as corn and sugarcane. Therefore, the biofuels has to be derived from the lignocellulose portion of biomass or in other words, the by-product or waste of agricultural activities to prevent the conflict of food source. Research shows that by supporting the second generation biofuel industry, which is being extracted from cellulosic biomass sources, by 2020; it can be commercially competitive to replace the first-generation ethanol that is generally made from corn [1]. Currently, there are several techniques available in the industry for the conversion of unwanted biomass to combustible, energy-packed fuel; nevertheless, pyrolysis appears to be a relatively promising technique in terms of its simplicity, production yield and economical value.

In recent years, fluidised beds have been extensively used as reactors for pyrolysis as they overcome some of the disadvantages of the conventional pyrolysis reactors such as fixed bed [2]. Fluidised beds have a comparably higher rate of reaction per unit volume due to the highly turbulent flow of the dense solid bed. The turbulence has promoted a better mixing environment for the biomass to have a higher heat transfer rate with the inert particles. One research reported that their designed reactor is able to reach an astounding rate of 1000 ºC/s [3]. The turbulent environment has also give rise to the even temperature distribution of the bed, which prevents the formation of local hot spots.

Bubbling fluidised beds have gained its rising popularity in the biochemical industry nowadays due to its even mixing capability and thermal distribution. Large quantities of experimental studies and numerical research have been conducted for different process parameters on pyrolysis; however, the hydrodynamics of the fluidised bed reactors are still not well understood yet due to the complexity of the particle interactions. Therefore, simulations using CFD stands out as a useful tool to study the fluidisation process and ultimately obtain the required parameters for specific operation.

In this study, a CFD model is developed to investigate the complex fluidisation process of particles in a fast pyrolysis fluidised bed reactor, where the required operational parameters are assessed for each condition of particle diameters and density. Later in this assessment feasibility of fluidisation will be evaluated.

2. Simulation Survey

In 2009 a three-dimensional (3D) and transient model was developed to simulate the particle fluid dynamics inside a fluidised bed reactor [4]. In the mentioned simulation, the author used an Eulerian multi-fluid approach to study the interaction between the three phases that consist of solid particles, flowing inert gas and liquid formed throughout the fluidising process. In other word kinetic theory of granular flow (KTGF) was used to describe the particulate phase; which means the solid phase was considered as a granular body that behaves like a fluid, but it is contained of certain volume of solid grains. K-epsilon turbulence model was implemented for the liquid phase to simulate the fluid flow pattern of liquid phase under turbulent condition. The effect of the superficial velocity on the velocity profiles of the other two phases was discussed in the mentioned research. The CFD simulation results have shown good agreement when compared with the experimental data for validation purpose and the authors have devised a conclusion, where the particle interaction and energy flow in three-phase fluidised bed reactors can be predicted via computational simulation [4].

Another research has performed the CFD simulation on the two-phase bubbling fluidised beds using both of the Eulerian and Lagrangian attempts to compare the feasibility and capability in predicting the particle flow behaviour [5]. The authors of this research have found that the Eulerian or two-fluid model (TFM) have shown greater agreement with the experimental results on the bubble possibility compare to Lagrangian or computational particle fluid dynamics (CPFD) model. All bubble possibilities predicted by the CPFD along the bed width are overestimated especially, when it is very close to the sidewall. Their simulations have also demonstrated that the CPFD model is not capable of predicting the bubble formation mechanism during the initialisation of the fluidisation process, whereas TFM have agreed well with the experimental result. However, TFM has its drawback at the computational time consumed, when it is compared with the CPFD model, which is critically important in the simulation of a large-scale industrial fluidised bed [5].

Other research on 3-Dimensional Eulerian granular model to study and validate the behaviour of the biomass and solid grains through fast pyrolysis process in a fluidised bed reactor was developed [3]. The authors have proposed the usage of Eulerian multi-fluid model to predict the velocity profile and volume fraction of the gas phase. The temperature distribution, velocity profile and biomass products were simulated and demonstrated to show the alignment with the experimental measurements. The comparison of experimental measurements and model predictions has shown a satisfying agreement on the accuracy and feasibility of the Eulerian multi-fluid model. The product

yields attained from the simulation were found to show good agreement with the bio-oil production yield from experiment [3].

Geldart was the pioneer to categorise the solid flow behaviour after it is fluidised into four different distinctive classes [6]. These classes are characterised and determined by the density difference between the granular particles and the fluidising agent gas and by the mean solid particle size [7]. Although the Geldart's scale is oldest measure of particle class, it is still the most popular and preferable scale used by the researchers for more than 40 years [6]. There are two extreme classes under this system, which are called groups C and D and they occupy each ends of the scale. Group C is very difficult to fluidise because the density difference is too little and the particle size is too small [7]. The group C particles will either flow out of the bed with the fluidising medium or it will just stay as fixed bed or the fluidised part that called grey zone, which is relatively small and difficult to control. On the other hand, group D is a spout able class, where a comparably high velocity surge of gas would force through the granular solid beds and form a void in the middle of the bed and a grain's fountain at the top of the void [7]. Under the spouting condition, some of the particles are transported by the gas surge to the highest point of the bed while other solid grains will forced downward around the spout [8]. Both of the conditions are not preferable as they are hard to control and the heating process will be uneven, causing deterioration in the bio-oil quality.

Another research has investigated the momentum exchange between all the phases involved in a three-phased bubbling fluidised bed [9]. The drag models of Syamlal O'Brien model, Hill Koch Ladd model, Gidaspow model, the representative unit cell (RUC) model and the Richardson Zaki model were all investigated in this work. Preliminary simulations of a two-dimensional (2D) fluidised reactor is conducted by this researcher to investigate and show the effect of using turbulence models in the simulations agreed well with experiments. The comparisons of different drag models were made in their work, which has proven that the entire drag model failed to predict the bubble formation at the centre of the fluidised bed. However, among all the models, the RUC and Gidaspow model have demonstrated a relatively greater matching with the experimental results. Besides, the author has focused on the simulations on the bubble behaviour in both 2D and 3D fluidised bed reactor that was subjected to a uniform inlet gas distribution. The simulations are compared to experiments performed on a fluidised bed, and the simulation results agree well according to bubble frequency [9].

K-epsilon (K-ε) turbulence model has been one of the most common models used in the CFD simulation of the fluidised bed to study the flow characteristics of particles and gas under turbulent flow conditions. However, comparing the use of K-ε and not using it on turbulence model was investigated and the result shows no apparent difference in fluidised bed simulation [10]. Both of their models have provided a satisfying accordance with the experimental results and the trend has shown the volume fraction is concentrated, as it gets closer to the wall, while the centre was relatively low in the fluidised bed. From the results obtained, the authors have concluded that the K-ε turbulence model have virtually no effect on the simulation results in predicting the flow pattern and velocity profile of the solid particles in fluidised beds, hence, turbulence model is not required for future researches [10].

3. Model description

In the present work on fluidising bed, an Euler-Eulerian approach (EE) will be used to define the TFM for a 3D transient simulation as Eulerian simulation consumed less computational power than any Lagrangian approaches. The solid bed materials that will be investigated in the simulation work are silica sand and stainless steel beads of uniform size. These two materials are both inert and able to resist corrosion so that no chemical reactions will be taken place between the biomass and the dense particles. The beads will be situated initially inside the fluidised bed column in static condition and formed a desired height in the bed. The gas phase will then be introduced from the bottom of the bed to initiate the fluidisation of these granular beads.

Nitrogen gas is chosen as the fluidising agent due to its inert properties that prevents any chance of combustion in the fluidised bed. Before entering the fluidised bed column, the nitrogen gas will have to flow through a perforated plate with a sieve size of 250 micrometres to ensure that the gas is

distributed evenly for better mixing environment. Table 1 shows the dimensional properties of simulated fluidised bed column.

The designed fluidised bed is compact enough to be placed on a bench, which is convenient for the research purpose of small-scale pyrolysis reactor. Stainless steel was chosen as the dense particle because of its high conductivity that might be effective for boosting the heat transfer rate. AISI 316 is a modified stainless steel that designed for resisting corrosion, which is highly suitable for the pyrolysis fluidised bed application because the solid particles will be constantly under turbulent interaction with the biomass compound such as bio-oil or volatiles that might be corrosive.

Table 1. Physical parameters of the fluidised bed Column

Descriptions	Specifications
Bed type	Bubbling
Shape	Cylindrical
Diameter	50 mm
Column Height	500 mm
Bed Heating Height	100 mm

Silica sand is the most common type of dense solid used by researchers for the study of fluidised bed because it has inert properties and is low cost. In this study, the sand particles will serve as the baseline to evaluate the feasibility of fluidising the stainless steel particles. The minimum fluidisation velocity will be compared in both scenarios and the required process parameters are expected to obtain through the analysis of the simulation results. The stainless steel particles used have a maximum protrusion of 2.5 μm, which is considered to be extremely low comparing to the mean diameter of 0.5 and 1.0 mm. Silica sand has an even smaller value of sphericity than the stainless steel with the same diameter. Therefore, both of the solid particles are considered to be spherical for the ease of calculation. As shown in Table 2, there will be two diameter settings for each type of solids, which add up to 4 kinds of scenarios with different materials and diameters. The objective of testing two different diameters is to investigate the effect of particle size on fluidisation parameters and their corresponding accuracy.

Table 2. Solid materials properties

Descriptions	Specifications	
Beads Type	Silica sand	Stainless Steel
Density (kg/m^3)	2680	7980
Shape	Spherical	Spherical
Diameter (mm)	0.5, 1.0	0.5, 1.0

As this work focuses on fluidisation process of the beads in the fluidised bed while being heated, no biomass grain was simulated in this research. The implementation of valid and reasonable boundary conditions is crucial for the computational domain to compute the governing equations. The inlet boundary condition is a uniform gas flow with constant superficial velocity, while the outlet condition is a pressure boundary with an atmospheric pressure of 1 bar. Gravitational acceleration of 9.81 m/s^2 is applied to demonstrate the fluidisation of solid phase using drag force exerted by flowing gas. The wall boundary condition is set to be free slip for both the solid phase and gas phase because there is no adhesion of gas or solid with the wall. According to the current literature, there will be significant collisions between the solid particles, thus a restitution coefficient with value of 0.95 will be introduced to the solid phase [11]. The solid volume fraction at initial condition is set to be 59.8%

of the static solid bed height. The boundary conditions are recorded in Table 3. Drag model of Gidaspow is used to describe the relationship of Reynolds number or velocity with the drag coefficient because it is reported that the Gidaspow model is the best correlation among the available model such as the Symlal O'Briens and Richardson Zaki [9]. In this research, the Gidaspow model has shown the closest agreement with the experimental results. The transient simulation of fluidisation will be run for a time period of 1 second for each settings of gas inlet velocity ranging from 10 to 150 cm/s to obtain the minimum fluidisation velocity and demonstrate the transformation of fluid behaviour during fluidisation.

Table 3. Process parameters and boundary conditions

Descriptions	Specifications
Gas Type	Nitrogen
Gas Velocity (cm/s)	10 – 150
Coefficient of Restitution	0.95
Drag Model	Gidaspow

Since it is concluded that turbulence model plays an insignificant role in the CFD simulation of fluidisation process, no turbulence model will be implemented to the granular flow simulation in the coming computational work [5], [10]. Initial simulations were validated by mesh refining method. Mesh size refined up to the limitation of research time and available computer speed. After observing of no significant change in the results, the optimum meshing size was chosen to run the rest of the simulation investigation.

4. Results and discussion

Fluidisation will only take place when the minimum fluidisation velocity is achieved or exceeded by the superficial velocity through the solid bed. In other words, the solid particles are fluidised when the nitrogen velocity is equal to the minimum fluidisation velocity. Hence, the minimum fluidisation velocity of a certain material with a specific diameter can be found by studying the changes of solid volume fraction over a period of time. When any drastic bed expansion or bubble formation is spotted from the volume fraction contour, the solid particles can confirmed to be successfully fluidised.

The fluidisation process can be indicated as shown in Figure 1, where the volume fraction of steel beads was monitored with varying velocity of nitrogen. Five different superficial velocities were simulated for the setting of steel particles with diameter of 0.5 mm at the flow time of 0.5 s. In other words, the volume fraction of steel beads at the timing of 0.5 s was captured for each gas velocities using the EE-TFM simulation. As shown in Figure 1, a conspicuous bubble can be seen forming at the middle of the solid bed, when the superficial velocity supplied is 70 cm/s. This is the first velocity that has shown the formation of bubble, when the velocity increased from 60 to 100 cm/s. Therefore, the minimum fluidisation velocity of steel particles with diameter of 0.5 mm can be concluded to be 70 cm/s.

From Figure 1, it can be seen that as the velocity of nitrogen applied increased, the hydrodynamics activity of the solid bed became more violent and turbulent. Before it reached the minimum fluidisation velocity, at the gas velocity of 60 cm/s, not a single bubble can be observed and no significant bed expansion can be seen. The solid particles were only at fixed bed condition, where the nitrogen merely flowed through the empty spaces between each particle without suspending or lifting any solids. When the minimum fluidisation velocity is achieved, a single large bubble can be seen forming at the bottom of the bed that is quickly flowing upward through the bed.

At the superficial velocity of 80 cm/s, after the minimum required velocity was achieved, it can be seen that a flat empty space was formed in the middle of the bed that does not touch the wall, instead of a circular bubble. The flat shaped gas bubble pushes that portion of the bed upward, resembling a

piston action, where the particles were raining down from the pushing slug formed and integrated with the remaining bed. A minor bed expansion can be observed from the velocity because of the empty void caused by the relatively large gas holdup as contrasting from the situation at 70 cm/s.

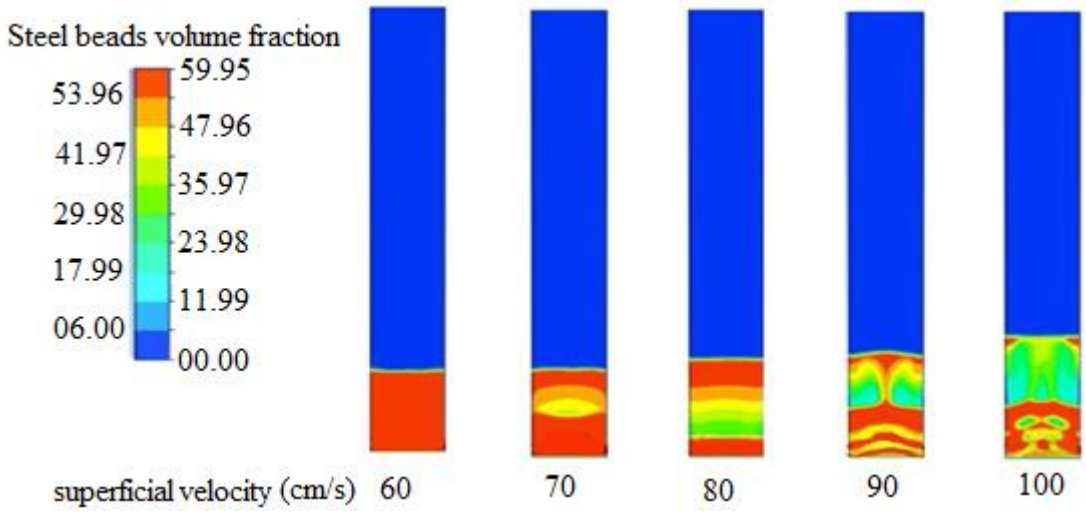

Figure 1. Volume fraction of steel beads when subjected to different gas superficial velocities (Steel, Diameter = 0.5 mm)

As the velocity increased by an extra 10 cm/s, an even greater empty space can be seen from Figure 1. However, instead of forming a flat gas void, an irregular shape of gas bubble was formed near the sides of the wall. It can be seen that the cycle time of bubble formation have been shortened as new bubbles have started to form at the bottom of the bed even before the top bubble escaped from the solid bed. At the highest tested velocity of 100 cm/s, a massive gas void can be spotted as the solid bed was pushed upward by the high pressure gas bubble or slug. The void has caused a comparably significant and large bed expansion.

During the fluidisation process, the velocity of the solid and gas phases change rapidly and drastically in different time and location in the solid bed. The velocity vector pattern for the 0.5 mm steel beads at 0.5 s was shown in Figure 2. It can be clearly seen that the solid flow was in symmetry structure and a two-directional circulation pattern, where it resembles the fluid flow during boiling state.

As shown in Figure 2, the centre area appeared to be a fast bubble flow region where the solid particles were pushed upward by the flow, while the sidewall region, the particles were flowing downward. There is a gas void region, where the steel velocity is zero emerging in the middle of the bed because of the gas bubble formation. The gas bubble was constantly flowing upward, which pushed the steel beads away from the bubble. The bubble movement resulted in the upward motion of steel beads right above the bubble and downward motion at the sides of the gas bubble.

At the bubble-free sidewall, the particles fell in a downward direction after being pushed by the central gas bubble. The bead gained velocity as it moved down the sides, resulting in a relatively high velocity zone that is marked by yellow and red arrows. In the area slightly lower than the high velocity zone, it can be seen that the steel beads were gaining higher velocity as a second bubble was forming at the bottom of the solid bed. It formed a triangular shaped region with upward velocity that is concentrated in the central area. The phenomenon is due to the collision between the falling particles and bubble-caused rising particles near the sidewall. Throughout all the simulation, the flow regime of the fluidisation process has appeared the same for different types of bed materials and varying diameters.

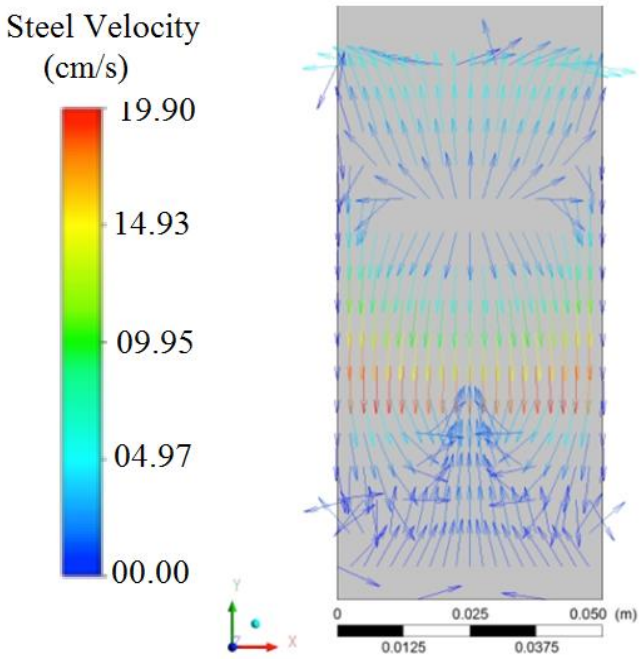

Figure 2. Velocity vector of steel beads during the bubble formation of
(Steel, Diameter = 0.5 mm, Superficial Velocity = 0.7 m/s, Time = 0.5 s)

As shown in Figure 3(a), only a single bubble was formed in a consistent cyclic timing, when the minimum fluidisation velocity is achieved. The width of the bubble is almost the same with the diameter of the fluidised bed column, stretching from one end of the wall to the other. This phenomena is called as slugging regime, where it is characterised by the formation of massive gas slugs with the size that is close to the cross-sectional area of the bed column [6].

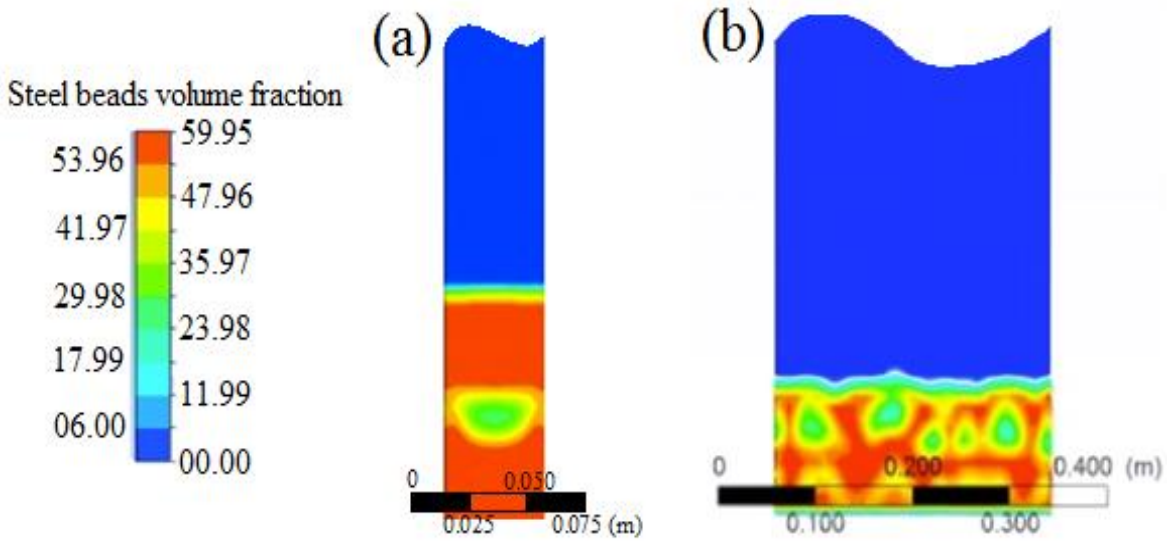

Figure 3. (a) slugging flow regime with a single large bubble formed in 50 mm diameter bed reactor and **(b)** bubbling flow regime in 300 mm diameter bed reactor (in both cases sand diameter is 1 mm and superficial velocity is 0.7 m/s)

As discussed, there are generally two types of slugging phenomena, where type A is a round-nosed gas bubble, while type B is a flat-nosed gas bubble, where the bubble appeared to be flatter at the top [6]. According to this research, the type B slug usually occurs with the bed materials that are more difficult to fluidise such as Group C. In other words, the findings from the simulation has confirmed the theoretical behaviour of group C particles have matched the simulation results, where bubble formed at the minimum fluidisation velocity and flat-nosed slug are more prone to happen with group C solid bed material.

It was also stated that a slugging phenomenon will only take place in fluidised bed that has a ratio of bed height to bed diameter that is larger than or equal to 2 [6]. In the current study, the bed height to bed diameter ratio is exactly 2, which explained why the slugging regime occurred in the designed fluidised bed column. Greater ratio of bed height to diameter provides sufficient time for the newly formed bubbles to fuse and coalesce into a larger bubble as shown in Figure 3(a), hence the bed diameter has to be increased to avoid any slugging regime to take place in the fluidised bed.

In order to test the above theory, a set of simulation was done by modifying the existing design of fluidised bed column. The bed diameter was increased 6 times from 50 mm to 300 mm, while the initial heating section of bed height was kept the same at 100 mm. As shown in Figure 3(b), many gas bubbles were formed instead of a single gas slug that observed in the original narrow column. Hence, from the results in Figure 3(b), it has proven that the slugging regime can be prevented by increasing the bed diameter. Slugging is not recommended or preferable as the flow regime for any fluidised bed application, namely pyrolysis because of the large bubble formation. The phenomena will cause a series of velocity surge in the solid particles as the large bubble pushes a portion of grains upwards with the bubble flow.

As the solid particles carried away by the bubble, it disrupted the heat distribution in the fluidisation system. Local hot spots might form near the sidewall where there is no formation of gas bubble. Hence, when biomass was fed into the fluidised bed, some of the biomass located at the central area will have a lower residence time as it is brought along by the slug; while the other biomass compound will flow slower, if it came near the side wall. It causes a deterioration in the bio-oil quality as portion of the biomass have been heated longer than the remaining compound, which has obsoleted the primary advantage of using a fluidised bed.

The graph of velocity magnitude of sand particles were plotted to monitor the velocity changes and patterns during the fluidisation process. As shown in Figure 4(a), when the sand particles were exposed to the inlet nitrogen velocity of 50 cm/s, a flat peak of velocity magnitude was observed at first 0.2 s. The velocity was first rose to a peak value of 0.025 m/s, and then it dropped slightly and stayed constant before diving to 0.015 m/s. The trend can be explained by the minor bed expansion and compaction, when the bed was introduced to the fluidising medium.

When the nitrogen gas first flowed into the bed, it causes the granular solid particles to move and make way for the gas to escape through the tiny empty spaces. It causes a surge in particle velocity that resulted in the peak shown in Figure 4(a); however, the gas velocity was not sufficient to sustain the weight of the sand beads, which causes the sand particles to slowly falling downward and the velocity to drop slightly.

As the solid particles fell and integrated with the bed, compaction took place, where the bed height returned to the quasi-steady state condition. After the quasi-steady state was achieved, the velocity magnitude of the sand particles became more or less stable and constant at 0.02 m/s. The same situation can be seen, when the superficial velocity was increased to 60 cm/s as shown in Figure 4(b). Nevertheless, a single peak of velocity magnitude was observed from the chart instead of the flat peak in lower superficial velocity.

The difference in the shape of peak can be explained by the shorter time taken by the higher velocity fluidised bed to achieve quasi-steady state condition. At higher superficial velocity, the solid particles reached the steady state in a relatively shorter time compare to lower velocity scenarios, as the drag force created by the gas flow is greater, when the velocity is higher. The drag force caused the sand particles to fall slower into the solid bed, resulting in a relatively lower velocity magnitude value

compare to Figure 4(a). It has also lessen the extent of the bed compaction process during the quasi-steady state condition, where the constant velocity magnitude is only 0.004 m/s as compared to the value of 0.020 m/s at the lower velocity in 0.5 s.

At the superficial velocity of 70 cm/s, the velocity magnitude pattern, as shown in Figure 4(c), has changed completely from the previous configurations. A consistent oscillatory pattern was observed with regular peaks of 0.013 m/s and a cyclic or peak to peak period of 0.3 seconds. The pattern indicated that the minimum fluidisation velocity has been achieved by the fluidising agent, where air bubbles were formed in the solid bed. The cyclic pattern of velocity magnitude was caused by the consistent formation of a single, large bubble throughout the fluidising process. As a bubble formed, it forced the particles to move upwards, which causes the velocity magnitude to peak at 0.1 seconds. Then, as the air bubble escaped from the solid bed, the velocity magnitude decreased, when the solid particles slowly rained down onto the top surface of the bed.

Almost immediately after the escape of the first gas bubble, the second bubble was formed at the bottom of the bed at around 0.25 seconds. The second bubble pushed the solid particles upward through the bed again and resulted in an increment of velocity similar to the first peak pattern. The velocity magnitude dropped once again, as the bubble disintegrated and the cycle continues endlessly with the same trend and similar process. A large bubble will form in every 0.3 seconds with a consistent frequency of 3.33 bubbles per second.

According to Geldart's scale, the sand particles with diameter of 1.0 mm can be considered as a Group C particle. The major characteristic of the particle class is that bubbles are formed at the minimum fluidisation velocity, where no intermediate stage of bed expansion happens during the process. The velocity magnitude pattern in Figure 4(c) can confirmed that the theory of Group C flow behaviour is true, where bubbles are formed consistently at the minimum fluidisation velocity itself. Hence, the fluidisation of any solid bed with different properties can be indicated from the corresponding granular velocity magnitude graph in future research. Whenever a cyclic pattern is observed from any Group C particles at a specific superficial velocity, it can be concluded that the solid bed have been fluidised. Besides, the minimum fluidisation velocity can be found without referring to and relying on the transient solid volume fraction contour to visually search for any visible gas bubble present in the solid bed.

Nevertheless, as the velocity increases beyond the minimum fluidisation velocity, a random pattern was exhibited by the solid particle velocity magnitude. As shown in Figure 4(d), when the superficial velocity was adjusted to 80 cm/s, which is above the minimum fluidisation velocity, the cyclic pattern have been distorted to demonstrate many different peaks with several irregular time intervals between each peaks. From the animation video of solid volume fraction with the superficial velocity of 80 cm/s, it has shown that bubbles were formed at a higher rate than the previous case of 70 cm/s. The rate was so high that some of the bubbles actually formed before the previous bubble escaped from the solid bed. Hence, it causes the cyclic pattern to be distorted as shown in Figure 4(d), where some of the cycles were overlapping with each other.

The overlapping conditions resulted in the forming of very high peak such as the highest velocity magnitude at 0.5 seconds, where it has reached 0.025 m/s, boosted almost double comparing to the highest peak of 0.013 m/s at the superficial velocity of 70 cm/s. It was due to the superposition of velocity magnitude that was caused by two bubbles that co-existed in the solid bed at the same time. However, the peaks were lowered as time went on because the formation of bubble has become more irregular. The increased formation rate of bubbles have lowered the possibility or chance of larger bubble to form because the flowing time was too short for the smaller bubbles to coalescence into a larger one before escaping the solid bed. Therefore, since the smaller bubbles were formed at different timings, it has rendered the velocity magnitude pattern to be seemingly more random than the usual case.

Same simulation runs were performed on both materials of choice for beads and two tested sizes with similar output behaviour but in different in range results.

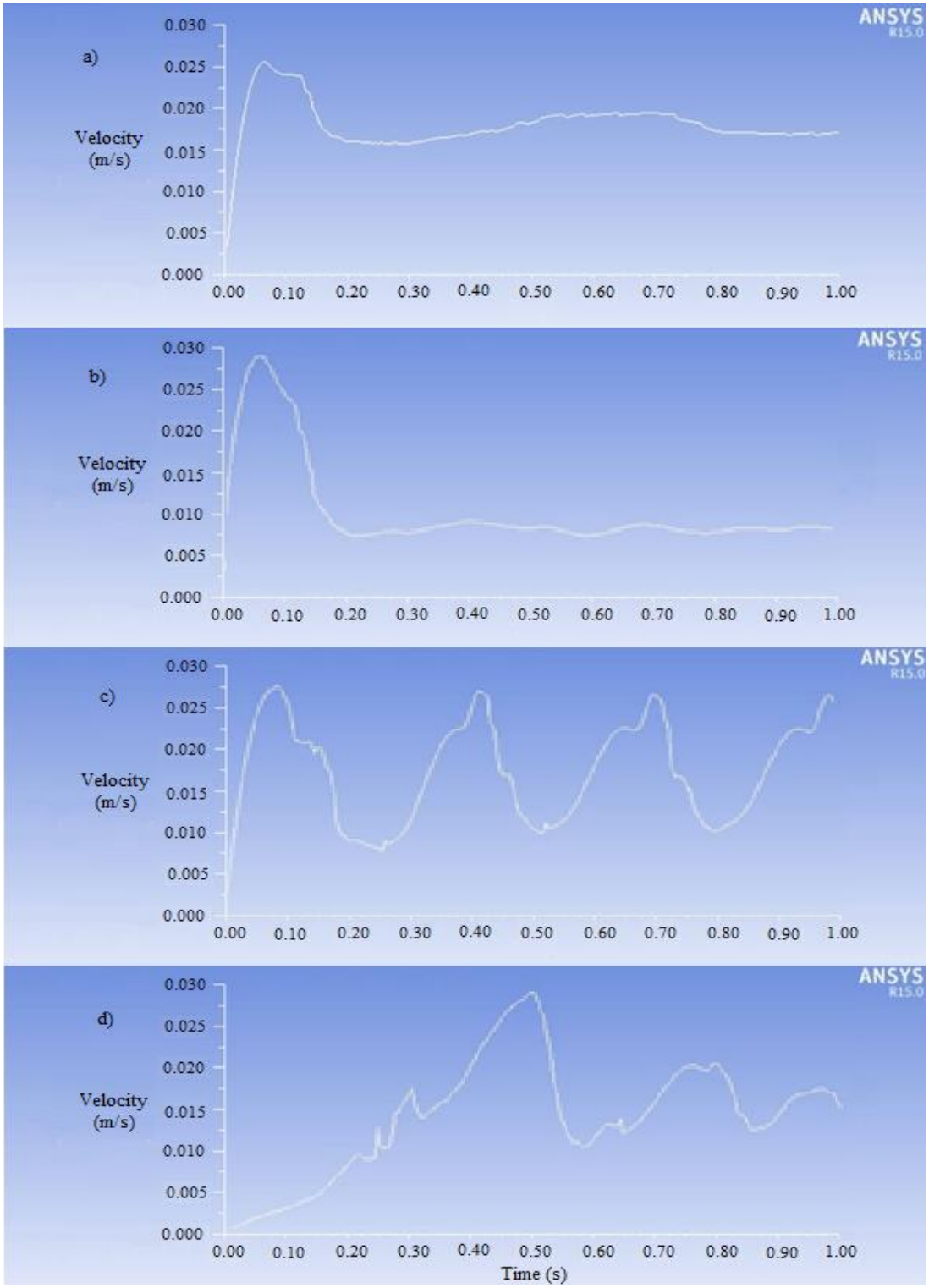

Figure 4. Velocity magnitude of 1.0 mm diameter sand beads against flow time
a) flat peak when superficial velocity is 0.5 m/s
b) single high peak before minimum fluidisation velocity when superficial velocity is 60 cm/s
c) cyclic pattern at the minimum fluidisation velocity when superficial velocity is 70 cm/s
d) random pattern when superficial velocity is 80 cm/s

5. Conclusions

In the present paper, the CFD simulation on the particle hydrodynamics of a two phase fluidised bed have been performed for two different bead materials with two different particle diameters. The Euler-Eulerian two-fluid model was deployed for the numerical simulation to study the fluidisation process and to obtain the minimum fluidisation velocity. Multiple hydrodynamics variables were studied in the ANSYS FLUENT simulation of fluidisation process, which includes the solid volume fraction distribution, the velocity magnitude fluctuation, bubble formation frequency and the velocity profile at different bed heights.

From the simulation, it has been found that the minimum fluidisation of steel beads can be achieved with nitrogen superficial velocities of 70 cm/s and 140 cm/s for diameter of 0.5 mm and 1.0 mm beads respectively. On the other hand, the minimum required superficial velocities to fluidise sand beads are 30 cm/s and 70 cm/s for particle diameter of 0.5 mm and 1.0 mm respectively. It has also discovered that the minimum fluidisation velocity will increase as the density of the particle material increases; while it will also increase when the particle diameter increases. Hence, it can be concluded that the drag force required to fluidise the specific material is proportional to both the density and the diameter of the particle chosen.

Slugging phenomena have been observed from every simulation settings as it often happened when the ratio of initial bed height to the fluidised bed column diameter is more than or equal to 2. Since the height to diameter ratio of the designed column in this research is exactly 2, the simulation results have proven that theory is applicable to the Euler-Eulerian two-fluid model of the fluidisation process. Furthermore, the results have exhibited strong agreement with the theoretical characteristics of the Geldart's scale group C particles, where the fluidisation of the group C particles can be indicated by formation of bubble without any significant bed expansion.

The velocity magnitude fluctuations have been studied, where it has been found that the pattern varies with the superficial velocity of the nitrogen as fluidising agent. Before approaching the minimum fluidisation velocity, the velocity magnitude of the solid particles will appeared to be stagnant after the first peak. However, a relatively uniform cyclic pattern will be observed as soon as the particles are fluidised with a slugging flow regime.

Although the simulation was validated by using mesh refining method, an experiment should be conducted in the future with accordance to the geometrical and operational parameters used in the simulation in order to validate the simulation results. The simulation can be improved by reducing the size of each time step based on time limits and computer's processor's speed. The refinement will yield a higher result resolution, which is essential for the prediction of fluidisation process and its application. Furthermore, the design of the fluidised bed column can be modified by enlarging the reactor diameter to prevent any slugging phenomenon, if the geometry of the practical furnace allows the above modification.

Acknowledgment

The authors would like to acknowledge the Centre for Biomass Research in INTI International University and faculty of Engineering of the University of Nottingham Malaysia Campus for their support towards this work.

References

[1] Stephen J, Mabee W and Saddler J 2011 Will second-generation ethanol be able to compete with first-generation ethanol? Opportunities for cost reduction *Biofuels, Bioproducts and Biorefining* **6(2)** pp 159–76

[2] Trambouze P and Euzen J 2005 Chemical reactors: from design to operation *Choice Reviews Online* **42(05)** p 283

[3] Mellin P, Zhang Q, Kantarelis E and Yang W 2013 An Euler–Euler approach to modeling biomass fast pyrolysis in fluidized-bed reactors – Focusing on the gas phase *Applied*

Thermal Engineering **58(1–2)** pp 344–53
[4] Panneerselvam R, Savithri S and Surender G 2009 CFD simulation of hydrodynamics of gas–liquid–solid fluidised bed reactor *Chemical Engineering Science* **64(6)** pp 1119–35
[5] Liang Y, Zhang Y, Li T and Lu C 2014 A critical validation study on CPFD model in simulating gas–solid bubbling fluidized beds *Powder Technology* **263** pp 121–34
[6] Yang W 2003 *Handbook of fluidization and fluid-particle systems* (New York: Marcel Dekker)
[7] Gupta C and Sathiyamoorthy D 1999 *Fluid bed technology in materials processing* (Boca Raton, Fla.: CRC Press)
[8] Kunii D and Levenspiel O 1991 *Fluidization engineering* (New York: Wiley)
[9] Lundberg J 2008 *CFD study of a bubbling fluidized bed* (Faculty of technology, Telemark University College)
[10] Wang S, Hao Z, Lu H, Yang Y, Xu P and Liu G 2012 Hydrodynamics modeling of particle rotation in bubbling gas fluidized beds *International Journal of Multiphase Flow* **39** pp 159–78
[11] Lohaa C, Chattopadhyayb H, and Chatterjee P K 2014 Effect of coefficient of restitution in Euler–Euler CFD simulation of fluidized-bed hydrodynamics *Particuology* **15** pp 170–7